EUROPEAN ORGANIZATION FOR NUCLEAR RESEARCH
CERN — BEAMS DEPARTMENT

CERN-BE-2010-002 RF

RF CHARACTERIZATION OF SUPERCONDUCTING SAMPLES

Tobias Junginger#, CERN, Geneva Switzerland and MPIK Heidelberg, Germany
Wolfgang Weingarten, CERN, Geneva, Switzerland
Carsten Welsch, Cockcroft Institute Warrington and University of Liverpool, United Kingdom

Abstract

At CERN a compact Quadrupole Resonator has been re-commissioned for the RF characterization of superconducting materials at 400 MHz. In addition the resonator can also be excited at multiple integers of this frequency. Besides *R*s it enables determination of the maximum RF magnetic field, the thermal conductivity and the penetration depth of the attached samples, at different temperatures. The features of the resonator will be compared with those of similar RF devices and first results will be presented.

CERN-BE-2010-002
01/09/2009

Presented at : the 14th International Conference on RF Superconductivity (SRF09 BERLIN – DRESDEN)

Geneva, Switzerland
September 2009

RF CHARACTERIZATION OF SUPERCONDUCTING SAMPLES*

Tobias Junginger#, CERN, Geneva Switzerland and MPIK Heidelberg, Germany
Wolfgang Weingarten, CERN, Geneva, Switzerland
Carsten Welsch, Cockcroft Institute Warrington and University of Liverpool, United Kingdom

Abstract

At CERN a compact Quadrupole Resonator has been re-commissioned for the RF characterization of superconducting materials at 400 MHz. In addition the resonator can also be excited at multiple integers of this frequency. Besides R_s it enables determination of the maximum RF magnetic field, the thermal conductivity and the penetration depth of the attached samples, at different temperatures. The features of the resonator will be compared with those of similar RF devices and first results will be presented.

INTRODUCTION

The surface resistance R_s of superconducting cavities operated in the TM_{010} mode can be obtained by measuring the unloaded quality factor Q_0

$$Q_0 = \frac{G}{R_s}, \qquad (1)$$

where G is the geometry factor of the cavity, only dependent on the cavity shape and not on its size or material. G can therefore be easily and accurately obtained by a numerical simulation.

R_S may vary strongly over the cavity surface and the value obtained is an average over the whole surface [1],

$$R_S = \frac{\int_S R_s |\boldsymbol{H}|^2 dS}{\int_S |\boldsymbol{H}|^2 dS}$$

A more convenient way consists of investigating small samples. They can be cheaply manufactured and easily duplicated.

RF cavities excited in the TE_{011} mode with a sample attached as the cover plate are often used for material characterization. The TE_{011} mode is the TE mode of third lowest resonant frequency, see Fig. 1.

It is chosen, because of its convenient field configuration.

- No magnetic field and therefore no RF currents across the joint, where the demountable end plate is attached to the cavity, see Fig. 1.
- The electrical field vanishes over the whole cavity surface, helping to avoid multipacting.

The shape of a cylindrical pill box cavity with radius R and length d can be optimized with respect to several parameters for a given resonant frequency f. The cavity could be optimized to minimum surface area (d/R = 1.306), minimum volume (d/R = 1.165) or a maximum peak surface field on the sample surface for a given stored energy U (d/R = 1.498). Often d/R and f are chosen by practical issues like the size and shape of an available cryostat.

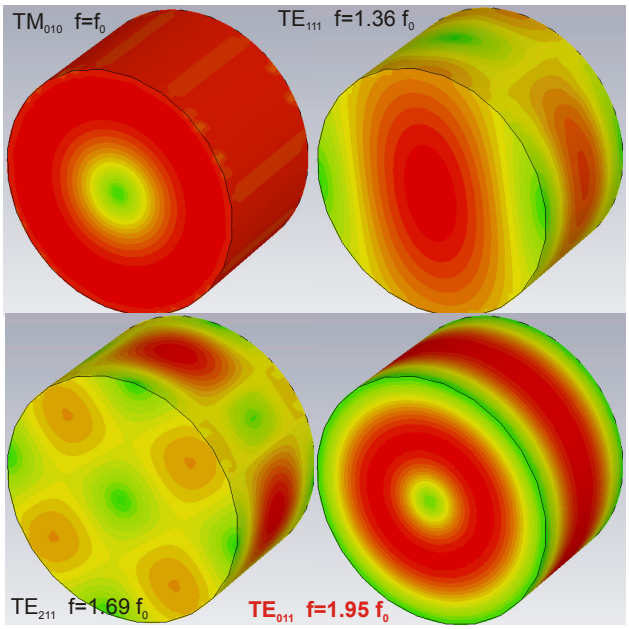

Fig. 1: False colour plots of resonant modes found in a cylindrical pillbox cavity optimized to lowest volume for a given resonant frequency in the TE_{011} mode (d/R = 1.165). The red/green color indicates areas of high/low magnetic field values. Displayed are the fundamental TM_{010} mode and the three TE modes of lowest resonant frequency.

Devices to Characterize Samples by RF

However, the pillbox geometry has always the drawbacks of having the same surface fields on the sample and the opposite endplate and impractical large size for the frequencies of interest concerning accelerator applications.

Therefore, besides the Quadrupole Resonator, several devices with modified shapes have been developed at various laboratories. In the following the main features of these instruments will be briefly mentioned, while a detailed description of each device can be found in the given reference.

A mushroom type cavity operated in a TE_{013} like mode enables to test samples with the maximum surface

*Work supported by the German Doctoral Students program of the Federal Ministry of Education and Research (BMBF)
#Tobias.Junginger@quasar-group.org

magnetic field on the sample being 75% higher than at any other spot on the whole cavity surface. To avoid an impractical large size and to be able to use common RF equipment the cavity is designed for an X-band resonant frequency [2].

A sapphire rod has been placed inside a pillbox cavity in order to lower its resonant frequency. The sample is thermally isolated from the cavity, allowing independent temperature control of the sample holder and the cavity. This is used for calorimetric measurements [3].

A third system uses instead of a demountable endplate a cylindrical sample composing a coaxial structure with its host TE_{011} cavity. This structure yields magnetic fields on the sample surface, which are 138 % higher than at any other spot on the cavity surface. In addition the samples can be used in a second system for further DC and RF measurements [4].

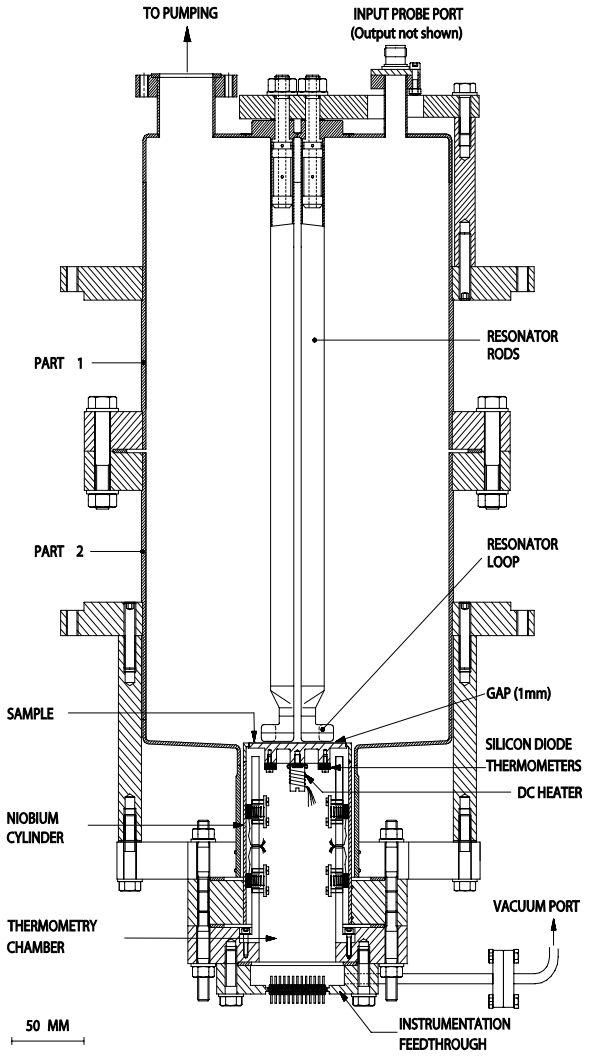

Fig. 2: Layout of the Quadrupole Resonator. The thermally isolated sample cylinder is illuminated by a four-wire transmission line and attached to the cavity in a coaxial structure [5].

THE QUADRUPOLE RESONATOR

The Quadrupole Resonator is a four-wire transmission line half-wave resonator using a TE_{21} like mode. The resonator was originally designed to measure the surface resistance of niobium film samples at 400 MHz, which are the technology and RF frequency chosen for the LHC at CERN. The sample is the cover plate of a cylinder attached to the cavity in a coaxial structure; see Fig. 2 [5].

Inside this structure the RF fields are exponentially decaying. This ensures that the power dissipated inside this structure and at the end flange and joint of the sample cylinder is negligible.

Furthermore the sample cylinder is thermally isolated from the cavity, enabling control of the sample temperature independently from the cavity temperature. For this purpose a DC heater and 6 silicon diodes have been placed inside the thermometry chamber.

The diodes have been calibrated using a three point correction to the standard curve as suggested by the manufacturer [6]. This gives an absolute accuracy of 100 mK for the temperature range between 1.4 and 10 K. The resolution is limited to 19 mK at 4 K due to a 12 bit digitalisation of the diode voltage, necessary for the data transfer.

The cavity itself is comprised of two 2 mm thick niobium cans for convenient handling and cleaning of the device. At the position where these cans are flanged together the screening current on the surface of the resonator vanishes.

The design considerations which led to the construction of the Quadrupole Resonator can be found in ref. 7, while the mechanical layout and the applied RF-DC compensation measurement technique are described in refs. 5 and 8.

Comparison with Other Devices

Table 1: Main specifications of four systems for the RF characterization of superconducting samples.

Device	Quadrupole Resonator	Sapphire loaded cavity	Mushroom cavity	Coaxial cavity
$\frac{B_{\mathrm{peak,sample}}}{B_{\mathrm{peak,cavity}}}$	1.2	1	1.75	2.38
f [GHz]	0.4	7.5	3.5	11.4
R [mm]	105	25	41.3/25	57.4
A [cm^2]	44	20	44	22
Calorimetric	Yes	Yes	No	No

The resonant frequency f of the Quadrupole Resonator of 400 MHz is significantly lower than those of the devices mentioned above, see Table 1. In spite of this relatively low frequency it is fairly compact compared to the other devices operated at a much larger frequency.

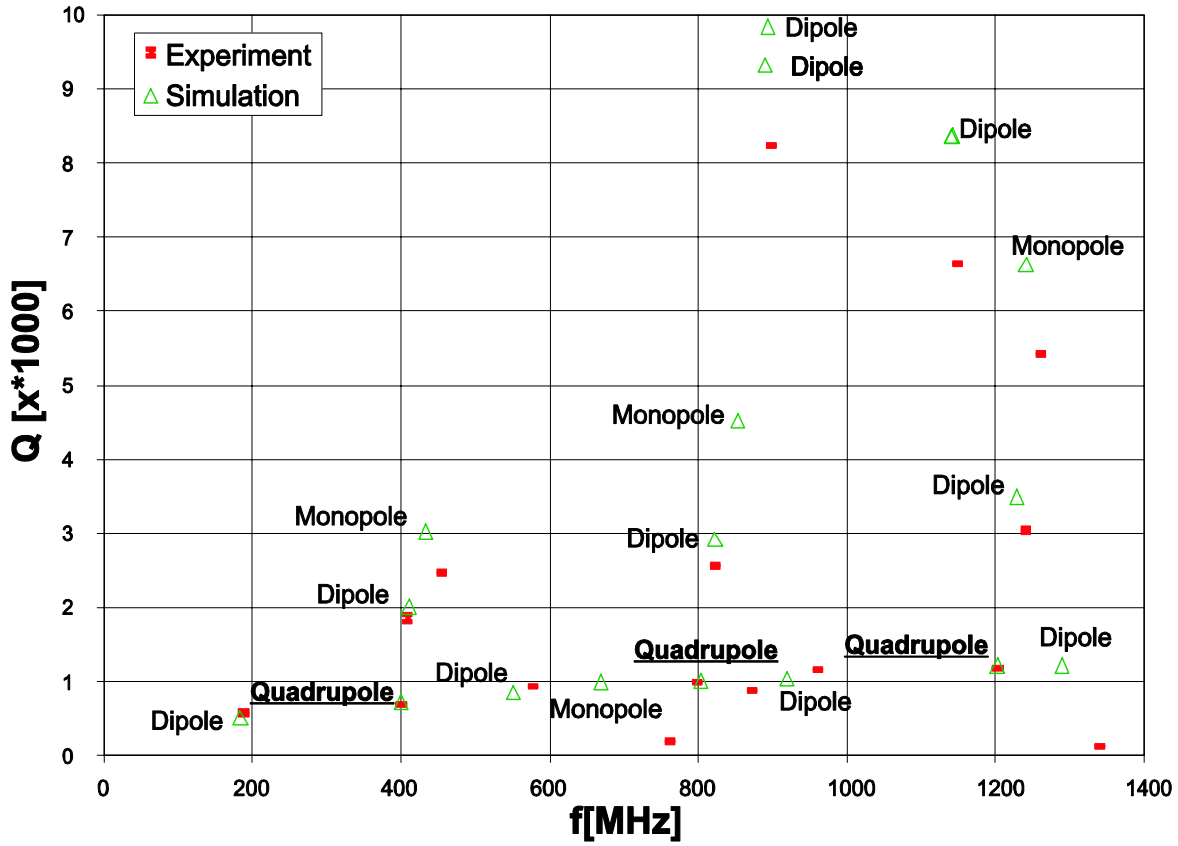

Fig. 3: Q-values at room temperature of resonant modes found in the Quadrupole Resonator. Only the quadrupole modes and the two dipole modes of lowest resonance frequencies are in cut-off in the gap between resonator and sample cylinder.

Calorimetric measurements can be performed with the Quadrupole Resonator and the Sapphire Loaded Cavity. These devices have lower ratios between the peak surface magnetic field on their samples $B_{peak,sample}$ compared to the peak surface magnetic field on the other parts of the cavity $B_{peak,cavity}$. But the independent control of cavity and sample temperature enables precise measurements, especially at relative high temperatures. For measurements at lowest temperatures, where the sample temperature shall not or only slightly exceed the bath temperature, the systems with higher ratio $B_{peak,sample}/B_{peak,cavity}$ are preferred.

The coaxial cavity is the only device using instead of flat samples a cylindrical sample. This geometry yields the highest ratio $B_{peak,sample}/B_{peak,cavity}$ amongst the resonators being compared here.

Resonant Modes

Simulations performed with CST Microwave Studio® show that multiple integers of the resonator's fundamental mode frequency of 400 MHz are also resonant frequencies of the device, see Fig. 3, as expected for a half-wave resonator.

This could be validated by measurements of the resonant frequencies using a spectrum analyzer. Besides the quadrupole modes at 400, 800 and 1200 MHz, there are also monopole and dipole modes found in the resonator. All the Q-values have been calculated using eq. 1 and

$$R_S = \frac{1}{\delta\sigma},$$

where the values of the penetration depth δ and the conductivity of niobium at room temperature σ are taken from the literature.

For all quadrupole modes and the two dipole modes of lowest resonant frequencies simulation and measurement results are in good agreement regarding Q-value and frequency.

All the other dipole modes are in fair agreement regarding the resonant frequency f. The maximum difference between simulation and measurement is 50 MHz for the dipole mode of highest frequency. The Q-value of these modes is systematically higher for the simulated values, due to the fact that all these modes have high field values in the gap between sample cylinder and cavity. Therefore the losses could not be accurately calculated due to the limited spatial resolution of the model.

The simulation predicts two dipole modes at 890 and 894 MHz with different field configurations and Q-values. At room temperature these two modes could not be separately resolved; only one resonance at 897 MHz was measured.

The monopole modes show the highest disagreement between measured and simulated values for the resonant frequency and Q-value. These modes are not in cut-off inside the coaxial structure between cavity and sample cylinder and have the highest field values in this gap and on the cover where the niobium rods are mounted to the cavity.

No further investigations on the monopole and dipole modes have been performed, since these modes are not interesting for the investigations of the samples. It is only important to know these modes in order to avoid their excitation.

The quadrupole modes at 800 and 1200 MHz however can be used for sample characterization.

FIRST RESULTS

First results on the Quadrupole Resonator were already published in 1998 [8] and 2003 [5]. In these publications the authors presented measurements of the surface resistance R_s as a function of temperature and applied magnetic field B on bulk Nb and Nb/Cu samples at f = 400 MHz.

The device has now been refurbished and here we present, besides results on R_s, measurements at 400 MHz of the maximum obtained RF field $B_{max,RF}$, the penetration depth λ and the thermal conductivity κ, performed on a reactor grade bulk niobium sample. Here we distinguish between $B_{max,RF}$, the maximum magnetic field obtained on the sample at a location, which a priori is unknown, and between B_{peak}, which denotes the maximum surface field at a precise location, as determined by computer codes.

Measurements at 800 and 1200 MHz are planned but have not been carried out so far.

Surface Resistance of the Sample

To determine the surface resistance of the attached sample as a function of applied magnetic field B, its distribution on the sample surface needs to be known. Since B^2 is proportional to the stored energy U, a constant c_1 can be defined for a given mode. Its value was calculated using CST Microwave Studio® for the quadrupole mode at 400 MHz:

$$c_1 = \frac{B_{peak}^2}{\omega U} = 4.14 \cdot 10^{-11} \frac{\mathrm{sT^2}}{\mathrm{J}}. \quad (2)$$

The loaded quality factor of a cavity Q_L equals

$$Q_L = \frac{\omega U}{P_L} = \omega\tau, \quad (3)$$

where P_L is the power dissipated in the cavity and the couplers, while τ is the decay time of the whole system comprising the cavity and the coupling ports.

If the coupling constant β = 1 as seen from the input coupler, the input power equals the output power yielding

$$P_i = P_t,$$

where P_i and P_t are the incident and transmitted powers, respectively.

For a strongly over-coupled system, like the Quadrupole Resonator, where the complete energy coupled to the system is almost completely coupled out instead of dissipated through the cavity walls, the following approximation can be made:

$$P_i = P_t = \frac{1}{2} P_L.$$

Transposing eq. 2 with respect to B_{peak} and substituting U using eq. 3 yields a simple expression for the peak surface magnetic field B_{peak} on the sample,

$$B_{peak} = \sqrt{2 c_1 \omega \tau P_i}. \quad (4)$$

B_{peak} can now be obtained by measurements of τ using a spectrum analyzer and P_i using a power meter.

The quality factor of the sample Q_{sample} can be written as a function of the surface resistance on the sample surface R_s and the geometry factor of the sample G_{sample}, which is calculated in the same manner as it would be for the whole cavity, but taking only into account the power dissipated in the sample. We obtain

$$Q_{Sample} = \frac{G_{Sample}}{R_S} = \frac{\omega U}{P_{diss}}, \quad (5)$$

where P_{diss} is the power dissipated on the sample surface due to RF heating. Substituting ωU by using the definition of c_1 (eq. 2) yields:

$$R_s = \frac{c_1 G_{sample} P_{diss}}{B_{max}^2}. \quad (6)$$

G_{sample} was calculated with CST Microwave Studio® and equals 214 Ω.

P_{diss} can be obtained by an RF-DC compensation measurement. For this purpose the sample is heated to the temperature of interest by a 1 kΩ resistor attached to its backside. Afterwards the RF is switched on. Now the DC current applied to the heater is lowered such as to keep the temperature of the sample constant. P_{diss} is derived from the difference between the DC power applied with and without the RF being switched on.

This measurement technique has already been used to measure R_s as a function of applied field of a chemically etched reactor grade bulk niobium sample at several temperatures, see Fig. 4.

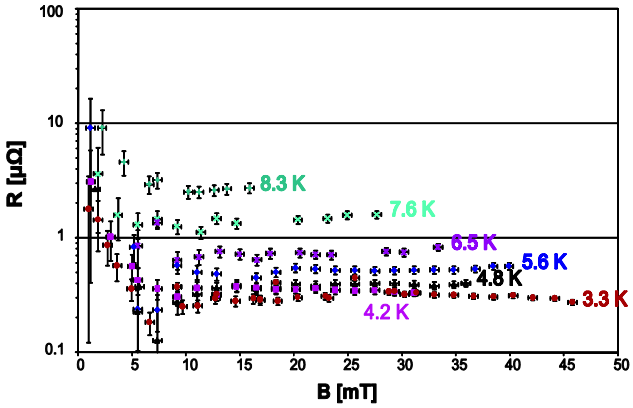

Fig. 4: Surface resistance of a chemically etched reactor grade bulk niobium sample as a function of the maximum applied magnetic field B for several temperatures.

The resolution was limited by the ampere-meter measuring the current applied to the DC heater (10 μA). For low fields this gives a poor resolution (82 nΩ at 4.2 K and 3.7 mT). For higher fields a resolution better than 1 nΩ could be obtained (0.93 nΩ at 4.2 K and 25 mT).

Some of the data at low temperature were measured using RF duty cycles < 1. This was necessary at higher fields; otherwise the temperature due to RF heating would have exceeded the temperature of interest.

Maximum RF Magnetic Field of the Sample

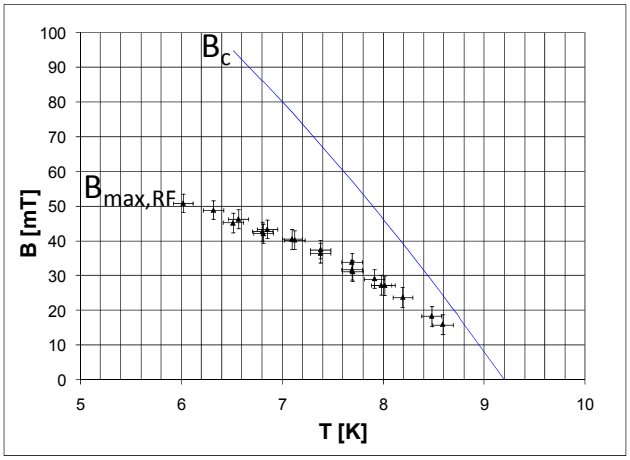

Fig. 5: Maximum RF field $B_{max,RF}$ and critical thermodynamic field B_c of Nb as a function of the temperature.

For the measurements of the maximum magnetic field $B_{max,RF}$ under RF exposure even shorter pulses were used. In this case one has to ensure that the heating due to the RF is negligible. This can be easily verified by measuring the temperature on the sample while the RF level is raised. Fig. 5 displays $B_{max,RF}$ as a function of temperature T.

The critical thermodynamic field B_c for niobium is displayed as well. It reads:

$$B_c(T) = B_c(0)\left[1 - \frac{T^2}{T_c^2}\right], \qquad (7)$$

$B_c(0) = 190$ mT.

Evidently, the measurement of the maximum magnetic field on the surface aims at the determination under RF exposure of the intrinsic critical magnetic field $B_{c,RF}$ of the sample material under study [9]. However, for doing this, it must be confirmed that the measured maximum RF field $B_{max,RF}$ on the sample is indeed limited by the $B_{c,RF}$ and not by the dissipation and restricted removal of the heat at a local defect. Therefore one needs criteria to distinguish between these alternatives.

Such criteria are provided by the different dependencies on the sample temperature of the limitation mechanisms. The limitation mechanisms can be either of magnetic or of thermal origin. For instance, for the magnetic limitation, $B_{max,RF}$ is proportional to the critical magnetic field, $B_{max,RF} \sim B_{c,RF} \sim 1 - (T/T_c)^2$, hence to the square of the temperature. In contrast, for the thermal limitation, the locally dissipated power $P_{diss} \sim B^2_{max,RF}$ goes linearly with the temperature, $B^2_{max,RF} \sim P_{diss} \sim 1 - (T/T_c)$. Hence whatever plot of either $B_{max,RF}$ vs. T^2 or $B^2_{max,RF}$ vs. T gives a straight line describes the physical reality.

This procedure was applied for the data as depicted in Fig. 5. The result, shown in Fig. 6, is consistent with a thermal limitation.

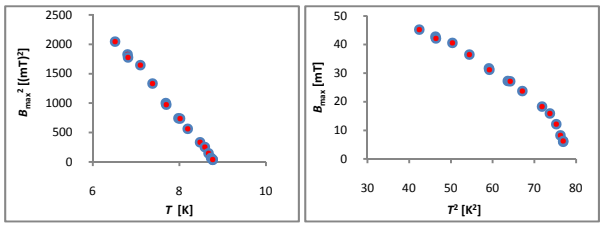

Fig. 6: Plot of data as shown in Fig. 5 to distinguish between a thermal (left) and a magnetic limitation (right). The left plot displays a straight line, which indicates that the limitation is of thermal origin.

Should it turn out that the limitation is of magnetic origin, for an accurate determination of $B_{c,RF}$ one needs to know where exactly on the sample the quench occurs and how the field at this position is correlated to the peak field on the sample B_{peak}. The quench could for example occur at a position where the field is lower than B_{peak} but the temperature is much higher.

The assumption is certainly correct that the quench occurs where the radial RF surface field $B(r)$ as determined when $B = B_{max,RF}$, comes closest to the critical field of Nb, $B_c\,(T(r))$. B_c depends via the temperature $T(r)$ on the radial position r.

Under this assumption the quench will occur at the position where the ratio between applied field $B(r)$ and $B_c\,(T(r))$ has a maximum. $B_c\,(T(r))$ can be calculated from

eq. 7 for an arbitrary position on the sample surface if the temperature $T(r)$ is known for every position r on this surface.

Thermal Conductivity of the Sample

Therefore the thermal conductivity $\kappa\,(T)$ of the sample as a function of temperature T was measured (Fig. 7). This could be done by DC heating the sample and determining T at two positions on the sample cylinder, while κ was then calculated from the temperature difference ΔT between the two spots.

The derived function $\kappa\,(T)$ can be used to calculate the temperature distribution $T\,(r)$ on the whole sample surface for a given temperature at the location of the diodes.

The magnetic field distribution $B\,(r)$ can be calculated using CST Microwave Studio®. Eq. 7 enables directly the determination of $B_c\,(T(r))$ for an arbitrary position on the sample surface from this temperature distribution and hence the critical field $B_{c,RF}\,(T)$.

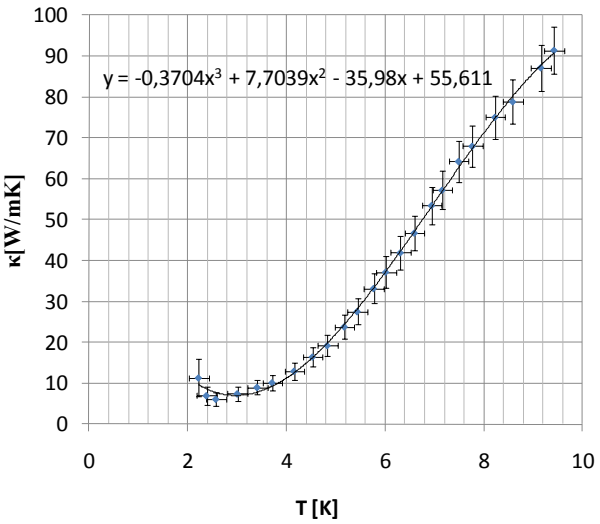

Fig. 7: Thermal conductivity $\kappa\,(T)$ of the niobium sample as a function of temperature. Within the displayed range $\kappa\,(T)$ can be approximated by a function of third order.

Penetration Depth of the Sample

The fact that the penetration depth λ changes rapidly with temperature for $T < T_c$ can be used for its measurement [10]. From the two fluid model with Pippard's correction for the mean free path l, the London penetration depth λ_L, the BCS coherence length ξ, and the critical temperature T_c, one can derive [11]:

$$\Delta\lambda = \lambda_L\sqrt{1+\frac{\xi}{l}}\cdot\left(\frac{1}{\sqrt{1-\left(\frac{T}{T_c}\right)^4}}-1\right). \qquad (8)$$

In case that ω varies only slowly with time ($\omega^{-2}\,d\omega/dt \ll 1$) an adiabatic invariant $I = U/\omega$ can be defined [12]. In this case the Slater theorem can be applied. It gives a relation between the changes of the stored energy U and the resonant frequency f of the cavity,

$$\frac{\Delta U}{U} = \frac{\Delta f}{f}\ .$$

For electric boundary condition ($\boldsymbol{n}\times\boldsymbol{E}=0$) it gives:

$$\frac{\Delta f}{f} = \frac{\frac{1}{4}\int_V(\epsilon_0\boldsymbol{E}^2-\mu_0\boldsymbol{H}^2)dV}{U} \qquad (9)$$

An increase of the penetration depth λ is equivalent to an increase of the cavity volume V. Therefore the volume change of the cavity ΔV can be expressed as a function of the sample surface area A and the change of penetration depth $dV = Ad\lambda$.

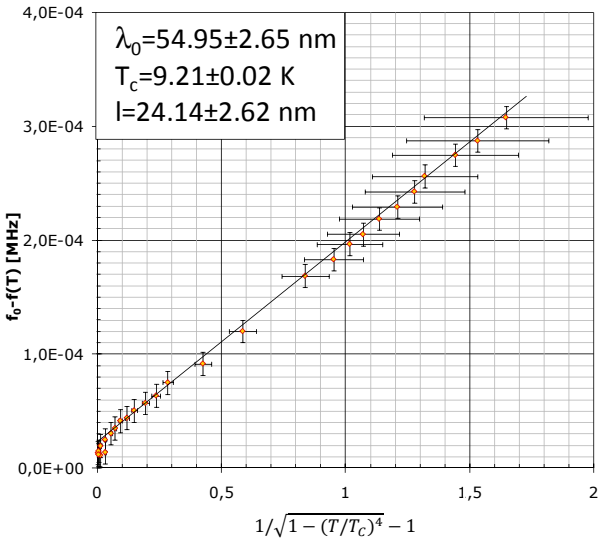

Fig. 8: The frequency shift is a linear function of the change in penetration depth $\Delta\lambda$. The parameters displayed in the box up left could be derived from the two fluid model with Pippard's correction (eq. 8).

This can be applied to eq. 8. Since the electric field $\boldsymbol{E}$ on the sample is small compared to the magnetic field ($\varepsilon_0 E^2 \ll \mu_0 H^2$) a further simplification can be made, yielding

$$\frac{\Delta f}{f} = -\frac{\frac{1}{4}\int_V\mu_0\boldsymbol{H}^2dV}{U}.$$

The stored energy U can be substituted using the definition of the G_{sample} and its quality factor Q_{sample} (eq. 5), yielding a linear relation between $\Delta\lambda$ and Δf,

$$\Delta\lambda = -\frac{G_{Sample}}{\pi\mu_0 f^2}\Delta f. \qquad (10)$$

The frequency shift Δf can be accurately measured using a frequency counter. The values obtained are displayed in Fig. 8.

The results have been fitted by applying eq. 8, while T_c, λ_0 and l where varied to obtain a mean square fit using the Levenberg-Malquardt algorithm, which can be applied to any non-linear fit [13]. The values of ξ and λ_L were taken from literature [1].

The fitting was performed using the WinSuperFit program, an extension of Halbritter's program [14].

The values of T_c and λ_0 are in good agreement with literature values. The low value of l is an indication for a dirty sample. This could also explain the relatively low value of the thermal conductivity, see previous section.

CONCLUSION

The Quadrupole Resonator enables the RF characterisation of superconducting samples. Compared to similar devices it has a very low resonant frequency, while its size is still relatively compact.

The device was initially built for measurements at 400 MHz, while multiple integers of this frequency are also resonant modes. Here we only published results obtained for a bulk niobium sample at 400 MHz. Measurements at 800 and 1200 MHz are planned for the future.

Experimental results on the surface resistance, the maximum RF field, the penetration depth and the thermal conductivity of a niobium sample have been described.

We observed low values for the maximum RF field and the mean free path. The origin of this shall be investigated by DC methods analyzing surface and thermodynamic properties of the sample.

ACKNOWLEDGMENT

The authors like to thank all the members of the BE/RF group and everybody else who contributed to the refurbishment of the Quadrupole Resonator. Special thanks go to G. Ciovati for providing us with the latest version of Halbritter's program to perform fits of our results.

One of us (TJ) is also indebted to the German Ministry of Education and Research for being awarded a grant by the German Doctoral Program at CERN (Gentner - Program).

REFERENCES

[1] H. Padamsee et al. - RF Superconductivity for Accelerators, John Wiley, New York 2008.

[2] A. Canabal et al. - Superconducting Material Testing with a High-Q Copper RF Cavity, Proceedings of PAC07, Albuquerque, New Mexico, USA.

[3] B. Xiao et al. - Commissioning of the SRF Surface Impedance Characterization System at Jefferson Lab, Proceedings of PAC09, Albuquerque, New Mexico, USA, Vancouver, Canada.

[4] G. Ciovati et al. - A Coaxial TE_{011} Cavity and a System to measure DC and RF Properties of Superconductors, Proceedings of SRF2007, Peking Univ., Beijing, China.

[5] E. Mahner et al. - A new instrument to measure the surface resistance of superconducting samples at 400 MHz, Rev. Scientific Instr. 7**4** (2003) 3390.

[6] B. C Dodrill et al. - Performance of Silicon Diode Temperature Sensors, Application of Cryogenic Technology, Vol. 10, 1991.

[7] E. Haebel et al. - The Quadrupole Resonator, design considerations and layout of a new instrument for the RF characterization of superconducting surface samples, Presented at EPAC-98, 6th European Particle Accelerator Conference, Stockholm.

[8] J.M. Tessier et al. - The Quadrupole Resonator: Construction, RF System , Field Calculations and first Applications, Presented at EPAC-98, 6th European Particle Accelerator Conference, Stockholm.

[9] T. Hayes et al. - Measuring The RF Critical Field of Pb, Nb, and Nb_3Sn, Presented at the 8th Workshop on RF Superconductivity and submitted to Particle Accelerators.

[10] W. Weingarten - Superconducting cavities, Proceedings of the Joint US-CERN-Japan International School on Frontiers of Accelerator Technology, Hayama/Tsukuba, Japan, 9 - 18 Sep. 1996, eds. I. Kurokawa, M. Month, S. Turner, Singapore, 1998.

[11] A. B. Pippard - An experimental and theoretical study of the relation between magnetic field and current in a superconductor, Proc. Royal Society **A216** (1953) 547.

[12] L.D Landau and E.M Lifshitz - Course of Theoretical Physics Volume 1, Mechanics, Pergamon Press, 1976.

[13] W. H. Press, S. A. Teukolsky, W. T. Vetterling, B. P. Flannery - Numerical Recipes in C++: the art of scientific computing, Cambridge Univ. Press, 2nd ed., 2002.

[14] G. Ciovati - Private communication; J. Halbritter, Externer Bericht 3/69-2 (Kernforschungszentrum, Karlsruhe, 1969); Externer Bericht 3/70-6 (Kernforschungszentrum, Karlsruhe, 1970); J. Halbritter, Z. Phys. **266** (1974) 209.